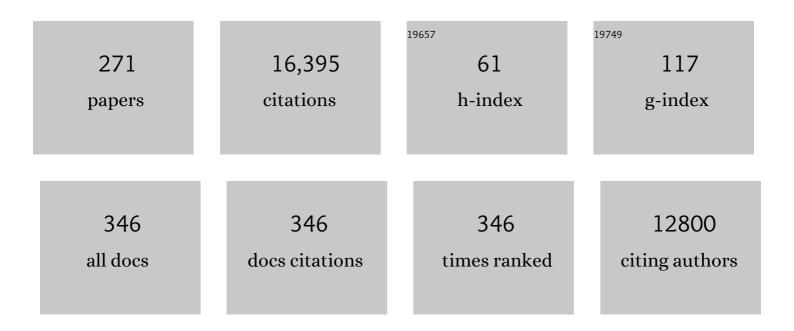
List of Publications by Year in descending order

Source: https://exaly.com/author-pdf/9558519/publications.pdf Version: 2024-02-01



#	Article	IF	CITATIONS
1	The role of the parenchymal vascular system in cerebrospinal fluid tracer clearance. European Radiology, 2023, 33, 656-665.	4.5	4
2	Threeâ€dimensional simultaneous brain mapping of T1,ÂT2, and magnetic susceptibility with MR Multitasking. Magnetic Resonance in Medicine, 2022, 87, 1375-1389.	3.0	15
3	Quantitative Susceptibility Mapping of Brain Iron Relating to Cognitive Impairment in Hypertension. Journal of Magnetic Resonance Imaging, 2022, 56, 508-515.	3.4	6
4	Automatic detection of neuromelanin and iron in the midbrain nuclei using a <scp>magnetic resonance imaging</scp> â€based brain template. Human Brain Mapping, 2022, 43, 2011-2025.	3.6	10
5	Brain iron deposition and movement disorders in hereditary haemochromatosis without liver failure: A crossâ€sectional study. European Journal of Neurology, 2022, , .	3.3	3
6	Vascular mapping of the human hippocampus using Ferumoxytol-enhanced MRI. NeuroImage, 2022, 250, 118957.	4.2	6
7	STAGE as a multicenter, multivendor protocol for imaging Parkinson's disease: a validation study on healthy controls. Chinese Journal of Academic Radiology, 2022, 5, 47-60.	0.6	4
8	Mapping Motor Pathways in Parkinson's Disease Patients with Subthalamic Deep Brain Stimulator: A Diffusion MRI Tractography Study. Neurology and Therapy, 2022, , 1.	3.2	2
9	A Comparison of Magnetic Resonance Imaging Methods to Assess Multiple Sclerosis Lesions: Implications for Patient Characterization and Clinical Trial Design. Diagnostics, 2022, 12, 77.	2.6	7
10	Quantitative susceptibility mapping of both ring and non-ring white matter lesions in relapsing remitting multiple sclerosis. Magnetic Resonance Imaging, 2022, 91, 45-51.	1.8	4
11	Plaque characteristics of middle cerebral artery assessed using strategically acquired gradient echo (STAGE) and vessel wall MR contribute to misery downstream perfusion in patients with intracranial atherosclerosis. European Radiology, 2021, 31, 65-75.	4.5	9
12	Imaging patients pre and post deep brain stimulation: Localization of the electrodes and their targets. Magnetic Resonance Imaging, 2021, 75, 34-44.	1.8	7
13	Quantitative MRI using STrategically Acquired Gradient Echo (STAGE): optimization for 1.5 T scanners and T1 relaxation map validation. European Radiology, 2021, 31, 4504-4513.	4.5	4
14	Quantitative susceptibility-weighted imaging may be an accurate method for determining stroke hypoperfusion and hypoxia of penumbra. European Radiology, 2021, 31, 6323-6333.	4.5	11
15	Fetal brain tissue characterization at 1.5 T using STrategically Acquired Gradient Echo (STAGE) imaging. European Radiology, 2021, 31, 5586-5594.	4.5	3
16	VC-Net: Deep Volume-Composition Networks for Segmentation and Visualization of Highly Sparse and Noisy Image Data. IEEE Transactions on Visualization and Computer Graphics, 2021, 27, 1301-1311.	4.4	21
17	Susceptibility-weighted Imaging: Technical Essentials and Clinical Neurologic Applications. Radiology, 2021, 299, 3-26.	7.3	92
18	An Overview of Venous Abnormalities Related to the Development of Lesions in Multiple Sclerosis. Frontiers in Neurology, 2021, 12, 561458.	2.4	13

#	Article	IF	CITATIONS
19	Imaging iron and neuromelanin simultaneously using a single 3D gradient echo magnetization transfer sequence: Combining neuromelanin, iron and the nigrosome-1 sign as complementary imaging biomarkers in early stage Parkinson's disease. NeuroImage, 2021, 230, 117810.	4.2	34
20	Assessing brain iron and volume of subcortical nuclei in idiopathic rapid eye movement sleep behavior disorder. Sleep, 2021, 44, .	1.1	12
21	All Central Nervous System Neuro- and Vascular-Communication Channels Are Surrounded With Cerebrospinal Fluid. Frontiers in Neurology, 2021, 12, 614636.	2.4	7
22	More on Exploiting the T1 Shinethrough and T2* Effects Using Multiecho Susceptibility-Weighted Imaging. American Journal of Neuroradiology, 2021, 42, E62-E63.	2.4	0
23	Estimating cerebral venous oxygenation in human fetuses with ventriculomegaly using quantitative susceptibility mapping. Magnetic Resonance Imaging, 2021, 80, 21-25.	1.8	2
24	Editorial: Quantitative Susceptibility Mapping in Neurodegeneration. Frontiers in Neuroscience, 2021, 15, 724550.	2.8	1
25	Utility of quantitative susceptibility mapping and diffusion kurtosis imaging in the diagnosis of early Parkinson's disease. NeuroImage: Clinical, 2021, 32, 102831.	2.7	9
26	Predicting Motor Outcome of Subthalamic Nucleus Deep Brain Stimulation for Parkinson's Disease Using Quantitative Susceptibility Mapping and Radiomics: A Pilot Study. Frontiers in Neuroscience, 2021, 15, 731109.	2.8	5
27	Dynamic Changes of Asymmetric Cortical Veins Relate to Neurologic Prognosis in Acute Ischemic Stroke. Radiology, 2021, 301, 210201.	7.3	6
28	Revealing vascular abnormalities and measuring small vessel density in multiple sclerosis lesions using USPIO. Neurolmage: Clinical, 2021, 29, 102525.	2.7	13
29	Quantifying Tissue Properties of the Optic Radiations Using Strategically Acquired Gradient Echo Imaging and Enhancing the Contrast Using Diamagnetic Susceptibility Weighted Imaging. American Journal of Neuroradiology, 2021, 42, 285-287.	2.4	1
30	Principles of susceptibility-weighted MRI. Advances in Magnetic Resonance Technology and Applications, 2021, 4, 341-357.	0.1	0
31	Editorial: Update on Vascular Contributions to Age-Related Neurodegenerative Diseases and Cognitive Impairment - Research of ISNVD 2020 Meeting. Frontiers in Neurology, 2021, 12, 797486.	2.4	1
32	Stability of AI-Enabled Diagnosis of Parkinson's Disease: A Study Targeting Substantia Nigra in Quantitative Susceptibility Mapping Imaging. Frontiers in Neuroscience, 2021, 15, 760975.	2.8	3
33	Reduced regional cerebral venous oxygen saturation is a risk factor for the cognitive impairment in hemodialysis patients: a quantitative susceptibility mapping study. Brain Imaging and Behavior, 2020, 14, 1339-1349.	2.1	11
34	Impact of nasopharyngeal irradiation and gadolinium administration on changes in T 1 signal intensity of the dentate nucleus in nasopharyngeal malignancy patients without intracranial abnormalities. Journal of Magnetic Resonance Imaging, 2020, 51, 250-259.	3.4	1
35	STrategically Acquired Gradient Echo (STAGE) imaging, part III: Technical advances and clinical applications of a rapid multi-contrast multi-parametric brain imaging method. Magnetic Resonance Imaging, 2020, 65, 15-26.	1.8	46
36	Visualizing the lateral habenula using susceptibility weighted imaging and quantitative susceptibility mapping. Magnetic Resonance Imaging, 2020, 65, 55-61.	1.8	18

#	Article	IF	CITATIONS
37	Dual-Imaging Modality Approach to Evaluate Cerebral Hemodynamics in Growth-Restricted Fetuses: Oxygenation and Perfusion. Fetal Diagnosis and Therapy, 2020, 47, 145-155.	1.4	3
38	Detecting sub-voxel microvasculature with USPIO-enhanced susceptibility-weighted MRI at 7ÂT. Magnetic Resonance Imaging, 2020, 67, 90-100.	1.8	13
39	Imaging the Nigrosome 1 in the substantia nigra using susceptibility weighted imaging and quantitative susceptibility mapping: An application to Parkinson's disease. NeuroImage: Clinical, 2020, 25, 102103.	2.7	63
40	Susceptibility and Volume Measures of the Mammillary Bodies Between Mild Cognitively Impaired Patients and Healthy Controls. Frontiers in Neuroscience, 2020, 14, 572595.	2.8	3
41	Multi-Echo Quantitative Susceptibility Mapping for Strategically Acquired Gradient Echo (STAGE) Imaging. Frontiers in Neuroscience, 2020, 14, 581474.	2.8	13
42	Imaging of the Spinal Cord in Multiple Sclerosis: Past, Present, Future. Brain Sciences, 2020, 10, 857.	2.3	10
43	Longitudinal Magnetic Resonance Imaging of Cerebral Microbleeds in Multiple Sclerosis Patients. Diagnostics, 2020, 10, 942.	2.6	3
44	Optimizing neuromelanin contrast in the substantia nigra and locus coeruleus using a magnetization transfer contrast prepared 3D gradient recalled echo sequence. NeuroImage, 2020, 218, 116935.	4.2	20
45	Prevention and control of COVID-19 in neurointerventional surgery: expert consensus from the Chinese Federation of Interventional and Therapeutic Neuroradiology (CFITN) and the International Society for Neurovascular Disease (ISNVD). Journal of NeuroInterventional Surgery, 2020, 12, 658-663.	3.3	10
46	Vascular, flow and perfusion abnormalities in Parkinson's disease. Parkinsonism and Related Disorders, 2020, 73, 8-13.	2.2	13
47	Subvoxel vascular imaging of the midbrain using USPIO-Enhanced MRI. NeuroImage, 2020, 220, 117106.	4.2	17
48	Strategically acquired gradient echo (STAGE)-derived MR angiography might be a superior alternative method to time-of-flight MR angiography in visualization of leptomeningeal collaterals. European Radiology, 2020, 30, 5110-5119.	4.5	3
49	Iron Content in Deep Gray Matter as a Function of Age Using Quantitative Susceptibility Mapping: A Multicenter Study. Frontiers in Neuroscience, 2020, 14, 607705.	2.8	20
50	Quantitative Susceptibility Mapping for Characterization of Intraplaque Hemorrhage and Calcification in Carotid Atherosclerotic Disease. Journal of Magnetic Resonance Imaging, 2020, 52, 534-541.	3.4	15
51	Rapid multicontrast brain imaging on a 0.35T MRâ€linac. Medical Physics, 2020, 47, 4064-4076.	3.0	21
52	The capability of detecting small vessels beyond the conventional MRI sensitivity using ironâ€based contrast agent enhanced susceptibility weighted imaging. NMR in Biomedicine, 2020, 33, e4256.	2.8	9
53	Radiomic Features of the Nigrosome-1 Region of the Substantia Nigra: Using Quantitative Susceptibility Mapping to Assist the Diagnosis of Idiopathic Parkinson's Disease. Frontiers in Aging Neuroscience, 2019, 11, 167.	3.4	52
54	Quantitative susceptibility mapping based hybrid feature extraction for diagnosis of Parkinson's disease. NeuroImage: Clinical, 2019, 24, 102070.	2.7	35

#	Article	IF	CITATIONS
55	Perfusion and Susceptibility Weighted Imaging in Traumatic Brain Injury. , 2019, , 303-319.		0
56	Regional High Iron in the Substantia Nigra Differentiates Parkinson's Disease Patients From Healthy Controls. Frontiers in Aging Neuroscience, 2019, 11, 106.	3.4	59
57	Cerebral microbleed detection using Susceptibility Weighted Imaging and deep learning. NeuroImage, 2019, 198, 271-282.	4.2	55
58	Venous and glymphatic drainage of the brain: Brief history of the International Society for Neurovascular Disease. Veins and Lymphatics, 2019, 8, .	0.1	0
59	The relation between cognitive dysfunction and diffusion tensor imaging parameters in traumatic brain injury. Brain Injury, 2019, 33, 355-363.	1.2	15
60	"Pseudo―T1-weighted appearance of the brain on FLAIR: unmasking the extent of gray matter involvement on susceptibility-weighted imaging in chronic toluene abuse. Neuroradiology, 2019, 61, 13-15.	2.2	1
61	Susceptibility mapping of the dural sinuses and other superficial veins in the brain. Magnetic Resonance Imaging, 2019, 57, 19-27.	1.8	5
62	Iron quantification in Parkinson's disease using an age-based threshold on susceptibility maps: The advantage of local versus entire structure iron content measurements. Magnetic Resonance Imaging, 2019, 55, 145-152.	1.8	18
63	Quantitative susceptibility mapping in the human fetus to measure blood oxygenation in the superior sagittal sinus. European Radiology, 2019, 29, 2017-2026.	4.5	13
64	Quantifying iron content in magnetic resonance imaging. Neurolmage, 2019, 187, 77-92.	4.2	71
65	Peripheral nerve magnetic resonance imaging. F1000Research, 2019, 8, 1803.	1.6	34
66	Screening of ligands for redox-active europium using magnetic resonance imaging. Bioorganic and Medicinal Chemistry, 2018, 26, 5274-5279.	3.0	7
67	Quantitative Flow Imaging in Human Umbilical Vessels In Utero Using Nongated 2D Phase Contrast MRI. Journal of Magnetic Resonance Imaging, 2018, 48, 283-289.	3.4	6
68	Reduced deep regional cerebral venous oxygen saturation in hemodialysis patients using quantitative susceptibility mapping. Metabolic Brain Disease, 2018, 33, 313-323.	2.9	7
69	The T1 shine through effect on susceptibility weighted imaging: an under recognized phenomenon. Neuroradiology, 2018, 60, 235-237.	2.2	11
70	Imaging putative foetal cerebral blood oxygenation using susceptibility weighted imaging (SWI). European Radiology, 2018, 28, 1884-1890.	4.5	12
71	Susceptibility weighted imaging and quantitative susceptibility mapping of the cerebral vasculature using ferumoxytol. Journal of Magnetic Resonance Imaging, 2018, 47, 621-633.	3.4	27
72	STrategically Acquired Gradient Echo (STAGE) imaging, part I: Creating enhanced T1 contrast and standardized susceptibility weighted imaging and quantitative susceptibility mapping. Magnetic Resonance Imaging, 2018, 46, 130-139.	1.8	76

#	Article	IF	CITATIONS
73	STrategically Acquired Gradient Echo (STAGE) imaging, part II: Correcting for RF inhomogeneities in estimating T1 and proton density. Magnetic Resonance Imaging, 2018, 46, 140-150.	1.8	42
74	Normal macromolecular clearance out of the ventricles is delayed in hydrocephalus. Brain Research, 2018, 1678, 337-355.	2.2	16
75	An interleaved sequence for simultaneous magnetic resonance angiography (MRA), susceptibility weighted imaging (SWI) and quantitative susceptibility mapping (QSM). Magnetic Resonance Imaging, 2018, 47, 1-6.	1.8	23
76	Quantification of liver iron concentration using the apparent susceptibility of hepatic vessels. Quantitative Imaging in Medicine and Surgery, 2018, 8, 123-134.	2.0	17
77	Subcortical brain iron deposition and cognitive performance in older women with breast cancer receiving adjuvant chemotherapy: A pilot MRI study. Magnetic Resonance Imaging, 2018, 54, 218-224.	1.8	12
78	A rapid, robust multi-echo phase unwrapping method for quantitative susceptibility mapping (QSM) using strategically acquired gradient echo (STAGE) data acquisition. , 2018, , .		3
79	1.5 Tesla Magnetic Resonance Imaging to Investigate Potential Etiologies of Brain Swelling in Pediatric Cerebral Malaria. American Journal of Tropical Medicine and Hygiene, 2018, 98, 497-504.	1.4	36
80	Susceptibilityâ€weighted imaging: current status and future directions. NMR in Biomedicine, 2017, 30, e3552.	2.8	121
81	Quantifying the changes in oxygen extraction fraction and cerebral activity caused by caffeine and acetazolamide. Journal of Cerebral Blood Flow and Metabolism, 2017, 37, 825-836.	4.3	33
82	Determination of detection sensitivity for cerebral microbleeds using susceptibilityâ€weighted imaging. NMR in Biomedicine, 2017, 30, e3551.	2.8	25
83	Susceptibility weighted imaging in acute cerebral ischemia: review of emerging technical concepts and clinical applications. Neuroradiology Journal, 2017, 30, 109-119.	1.2	29
84	Oxidation-Responsive, Eu ^{II/III} -Based, Multimodal Contrast Agent for Magnetic Resonance and Photoacoustic Imaging. ACS Omega, 2017, 2, 800-805.	3.5	22
85	<i>In vivo</i> imaging of prodromal hippocampus CA1 subfield oxidative stress in models of Alzheimer disease and Angelman syndrome. FASEB Journal, 2017, 31, 4179-4186.	0.5	34
86	Jugular Anomalies in Multiple Sclerosis Are Associated with Increased Collateral Venous Flow. American Journal of Neuroradiology, 2017, 38, 1617-1622.	2.4	12
87	Decreased susceptibility of major veins in mild traumatic brain injury is correlated with post-concussive symptoms: A quantitative susceptibility mapping study. NeuroImage: Clinical, 2017, 15, 625-632.	2.7	19
88	Amide proton transfer magnetic resonance imaging in detecting intracranial hemorrhage at different stages: a comparative study with susceptibility weighted imaging. Scientific Reports, 2017, 7, 45696.	3.3	30
89	MR imaging findings in mild traumatic brain injury with persistent neurological impairment. Magnetic Resonance Imaging, 2017, 37, 243-251.	1.8	40
90	COnstrained Data Extrapolation (CODE): A new approach for high definition vascular imaging from low resolution data. Magnetic Resonance Imaging, 2017, 44, 111-118.	1.8	2

#	Article	IF	CITATIONS
91	Structural Features of Europium(II) ontaining Cryptates That Influence Relaxivity. Chemistry - A European Journal, 2017, 23, 15404-15414.	3.3	39
92	Cover Image, Volume 30, Issue 4. NMR in Biomedicine, 2017, 30, i.	2.8	1
93	Increased susceptibility of asymmetrically prominent cortical veins correlates with misery perfusion in patients with occlusion of the middle cerebral artery. European Radiology, 2017, 27, 2381-2390.	4.5	24
94	Detecting prostate cancer and prostatic calcifications using advanced magnetic resonance imaging. Asian Journal of Andrology, 2017, 19, 439.	1.6	9
95	Ferritin–EGFP Chimera as an Endogenous Dual-Reporter for Both Fluorescence and Magnetic Resonance Imaging in Human Glioma U251 Cells. Tomography, 2017, 3, 1-8.	1.8	7
96	Compensation through Functional Hyperconnectivity: A Longitudinal Connectome Assessment of Mild Traumatic Brain Injury. Neural Plasticity, 2016, 2016, 1-13.	2.2	50
97	A quantitative study of susceptibility and additional frequency shift of three common materials in MRI. Magnetic Resonance in Medicine, 2016, 76, 1263-1269.	3.0	5
98	Susceptibilityâ€Weighted Imaging of Glioma: Update on Current Imaging Status and Future Directions. Journal of Neuroimaging, 2016, 26, 383-390.	2.0	54
99	A longitudinal study of placental perfusion using dynamic contrast enhanced magnetic resonance imaging in murine pregnancy. Placenta, 2016, 43, 90-97.	1.5	16
100	The connectivity domain: Analyzing resting state fMRI data using feature-based data-driven and model-based methods. NeuroImage, 2016, 134, 494-507.	4.2	69
101	Connectome-scale assessment of structural and functional connectivity in mild traumatic brain injury at the acute stage. Neurolmage: Clinical, 2016, 12, 100-115.	2.7	35
102	Validation of a Hemodynamic Model for the Study of the Cerebral Venous Outflow System Using MR Imaging and Echo-Color Doppler Data. American Journal of Neuroradiology, 2016, 37, 2100-2109.	2.4	13
103	Vestibular, balance, microvascular and white matter neuroimaging characteristics of blast injuries and mild traumatic brain injury: Four case reports. Brain Injury, 2016, 30, 1501-1514.	1.2	20
104	Assessing global and regional iron content in deep gray matter as a function of age using susceptibility mapping. Journal of Magnetic Resonance Imaging, 2016, 44, 59-71.	3.4	56
105	The phase value of putamen measured by susceptibility weighted images in Parkinson's disease and in other forms of Parkinsonism: a correlation study with F18 FP-CIT PET. Acta Radiologica, 2016, 57, 852-860.	1.1	3
106	A fully flow-compensated multiecho susceptibility-weighted imaging sequence: The effects of acceleration and background field on flow compensation. Magnetic Resonance in Medicine, 2016, 76, 478-489.	3.0	26
107	Grading of Gliomas by Using Monoexponential, Biexponential, and Stretched Exponential Diffusion-weighted MR Imaging and Diffusion Kurtosis MR Imaging. Radiology, 2016, 278, 496-504.	7.3	184
108	Susceptibility Weighted Imaging and Mapping of Micro-Hemorrhages and Major Deep Veins after Traumatic Brain Injury. Journal of Neurotrauma, 2016, 33, 10-21.	3.4	37

#	Article	IF	CITATIONS
109	Database integration of protocol-specific neurological imaging datasets. Neurolmage, 2016, 124, 1220-1224.	4.2	8
110	Susceptibility mapping of air, bone, and calcium in the head. Magnetic Resonance in Medicine, 2015, 73, 2185-2194.	3.0	48
111	Evaluating the Role of Reduced Oxygen Saturation and Vascular Damage in Traumatic Brain Injury Using Magnetic Resonance Perfusion-Weighted Imaging and Susceptibility-Weighted Imaging and Mapping. Topics in Magnetic Resonance Imaging, 2015, 24, 253-265.	1.2	11
112	A Eu ^{II} â€Containing Cryptate as a Redox Sensor in Magnetic Resonance Imaging of Living Tissue. Angewandte Chemie - International Edition, 2015, 54, 14398-14401.	13.8	64
113	Retrobulbar magnetic resonance angiography using binomial offâ€resonant rectangular (BORR) pulse. Magnetic Resonance in Medicine, 2015, 74, 1050-1056.	3.0	3
114	Jugular Venous Flow Abnormalities in Multiple Sclerosis Patients Compared to Normal Controls. Journal of Neuroimaging, 2015, 25, 600-607.	2.0	25
115	The role of magnetic resonance imaging in assessing venous vascular abnormalities in the head and neck: a demonstration of cerebrospinal venous insufficiency in a subset of multiple sclerosis patients. Veins and Lymphatics, 2015, 4, .	0.1	6
116	Cerebral Hemodynamic Changes of Mild Traumatic Brain Injury at the Acute Stage. PLoS ONE, 2015, 10, e0118061.	2.5	95
117	Improving Signal-to-Noise Ratio in Susceptibility Weighted Imaging: A Novel Multicomponent Non-Local Approach. PLoS ONE, 2015, 10, e0126835.	2.5	21
118	A Novel Multiparametric Approach to 3D Quantitative MRI of the Brain. PLoS ONE, 2015, 10, e0134963.	2.5	31
119	An improved method for susceptibility and radius quantification of cylindrical objects from MRI. Magnetic Resonance Imaging, 2015, 33, 420-436.	1.8	15
120	Resting State Functional Connectivity in Mild Traumatic Brain Injury at the Acute Stage: Independent Component and Seed-Based Analyses. Journal of Neurotrauma, 2015, 32, 1031-1045.	3.4	122
121	Quantifying errors in flow measurement using phase contrast magnetic resonance imaging: comparison of several boundary detection methods. Magnetic Resonance Imaging, 2015, 33, 185-193.	1.8	34
122	Quantifying brain iron deposition in patients with Parkinson's disease using quantitative susceptibility mapping, R2 and R2*. Magnetic Resonance Imaging, 2015, 33, 559-565.	1.8	215
123	Susceptibility-Weighted Imaging and Quantitative Susceptibility Mapping. , 2015, , 161-172.		2
124	Quantitative measurement of brain iron deposition in patients with haemodialysis using susceptibility mapping. Metabolic Brain Disease, 2015, 30, 563-571.	2.9	28
125	Striatal Iron Content Predicts Its Shrinkage and Changes in Verbal Working Memory after Two Years in Healthy Adults. Journal of Neuroscience, 2015, 35, 6731-6743.	3.6	92
126	Thickness of soft tissue of lower extremities measured with magnetic resonance imaging as a new indicator for staging unilateral secondary lower extremity lymphedema. Acta Radiologica, 2015, 56, 1016-1024.	1.1	9

#	Article	IF	CITATIONS
127	Susceptibility and size quantification of small human veins from an MRI method. Magnetic Resonance Imaging, 2015, 33, 1191-1204.	1.8	9
128	Quantitative measurements of brain iron deposition in cirrhotic patients using susceptibility mapping. Acta Radiologica, 2015, 56, 339-346.	1.1	18
129	Quantitative susceptibility mapping: current status and future directions. Magnetic Resonance Imaging, 2015, 33, 1-25.	1.8	426
130	Patterns of chronic venous insufficiency in the dural sinuses and extracranial draining veins and their relationship with white matter hyperintensities for patients with Parkinson's disease. Journal of Vascular Surgery, 2015, 61, 1511-1520.e1.	1.1	57
131	Traumatic Brain Injury by a Closed Head Injury Device Induces Cerebral Blood Flow Changes and Microhemorrhages. Journal of Clinical Imaging Science, 2015, 5, 52.	1.1	11
132	Automated White Matter Hyperintensity Detection in Multiple Sclerosis Using 3D T2 FLAIR. International Journal of Biomedical Imaging, 2014, 2014, 1-7.	3.9	15
133	MR venography of the fetal brain using susceptibility weighted imaging. Journal of Magnetic Resonance Imaging, 2014, 40, 949-957.	3.4	19
134	Improved MR venography using quantitative susceptibility-weighted imaging. Journal of Magnetic Resonance Imaging, 2014, 40, 698-708.	3.4	38
135	Is There Chronic Brain Damage in Retired NFL Players? Neuroradiology, Neuropsychology, and Neurology Examinations of 45 Retired Players. Sports Health, 2014, 6, 384-395.	2.7	91
136	Quantitative T2 Changes and Susceptibility-Weighted Magnetic Resonance Imaging in Murine Pregnancy. Gynecologic and Obstetric Investigation, 2014, 78, 33-40.	1.6	9
137	Measuring venous blood oxygenation in fetal brain using susceptibilityâ€weighted imaging. Journal of Magnetic Resonance Imaging, 2014, 39, 998-1006.	3.4	31
138	Recommendations for Multimodal Noninvasive and Invasive Screening for Detection of Extracranial Venous Abnormalities Indicative of Chronic Cerebrospinal Venous Insufficiency: A Position Statement of the International Society for Neurovascular Disease. Journal of Vascular and Interventional Radiology, 2014, 25, 1785-1794.e17.	0.5	57
139	Decreased oxygen saturation in asymmetrically prominent cortical veins in patients with cerebral ischemic stroke. Magnetic Resonance Imaging, 2014, 32, 1272-1276.	1.8	66
140	New DCE-MRI parameters to quantify the vascular changes induced by sunitinib treatment in renal carcinoma tumors. , 2014, , .		1
141	A Pilot Study of Hypofractionated Stereotactic Radiation Therapy and Sunitinib in Previously Irradiated Patients With Recurrent High-Grade Glioma. International Journal of Radiation Oncology Biology Physics, 2014, 90, 369-375.	0.8	22
142	Quantitative susceptibility mapping of small objects using volume constraints. Magnetic Resonance in Medicine, 2013, 69, 716-723.	3.0	20
143	A comparative study of magnetic resonance venography techniques for the evaluation of the internal jugular veins in multiple sclerosis patients. Magnetic Resonance Imaging, 2013, 31, 1668-1676.	1.8	15
144	MR imaging of the yucatan pig head and neck vasculature. Journal of Magnetic Resonance Imaging, 2013, 38, 641-649.	3.4	14

9

#	Article	IF	CITATIONS
145	Tissue similarity maps (TSMs): A new means of mapping vascular behavior and calculating relative blood volume in perfusion weighted imaging. Magnetic Resonance Imaging, 2013, 31, 481-489.	1.8	13
146	Measuring iron in the brain using quantitative susceptibility mapping and X-ray fluorescence imaging. NeuroImage, 2013, 78, 68-74.	4.2	144
147	Catalytic multiecho phase unwrapping scheme (CAMPUS) in multiecho gradient echo imaging: Removing phase wraps on a voxelâ€byâ€voxel basis. Magnetic Resonance in Medicine, 2013, 70, 117-126.	3.0	35
148	The Role of Hippocampal Iron Concentration and Hippocampal Volume in Age-Related Differences in Memory. Cerebral Cortex, 2013, 23, 1533-1541.	2.9	83
149	Noncontrastâ€enhanced magnetic resonance angiography and venography imaging with enhanced angiography. Journal of Magnetic Resonance Imaging, 2013, 38, 1539-1548.	3.4	26
150	Direct Portal Vein Thrombosis Visualization with T2*-Weighted Magnetic Resonance Imaging. International Journal of Medical Sciences, 2013, 10, 1570-1574.	2.5	4
151	Evaluating Hemorrhage in Renal Cell Carcinoma Using Susceptibility Weighted Imaging. PLoS ONE, 2013, 8, e57691.	2.5	22
152	In Vivo Measurement of Oxygenation Changes after Stroke Using Susceptibility Weighted Imaging Filtered Phase Data. PLoS ONE, 2013, 8, e63013.	2.5	31
153	Assessment of Intratumoral Micromorphology for Patients with Clear Cell Renal Cell Carcinoma Using Susceptibility-Weighted Imaging. PLoS ONE, 2013, 8, e65866.	2.5	4
154	Magnetic resonance imaging signatures of vascular pathology in multiple sclerosis. Neurological Research, 2012, 34, 780-792.	1.3	26
155	Characteristics of flow through the internal jugular veins at cervical C2/C3 and C5/C6 levels for multiple sclerosis patients using MR phase contrast imaging. Neurological Research, 2012, 34, 802-809.	1.3	32
156	Quantitative Flow Measurements in the Internal Jugular Veins of Multiple Sclerosis Patients Using Magnetic Resonance Imaging. Reviews on Recent Clinical Trials, 2012, 7, 117-126.	0.8	27
157	The Role of Venous Abnormalities in Neurological Disease. Reviews on Recent Clinical Trials, 2012, 7, 100-116.	0.8	23
158	Using Magnetic Resonance Imaging as a Means to Study Chronic Cerebral Spinal Venous Insufficiency in Multiple Sclerosis Patients. Techniques in Vascular and Interventional Radiology, 2012, 15, 101-112.	1.0	23
159	Blast-Induced Tinnitus and Hearing Loss in Rats: Behavioral and Imaging Assays. Journal of Neurotrauma, 2012, 29, 430-444.	3.4	91
160	The role of susceptibility weighted imaging in functional MRI. NeuroImage, 2012, 62, 923-929.	4.2	21
161	Imaging of stroke: a comparison between X-ray fluorescence and magnetic resonance imaging methods. Magnetic Resonance Imaging, 2012, 30, 1416-1423.	1.8	15
162	Patients with Multiple Sclerosis with Structural Venous Abnormalities on MR Imaging Exhibit an Abnormal Flow Distribution of the Internal Jugular Veins. Journal of Vascular and Interventional Radiology, 2012, 23, 60-68.e3.	0.5	61

#	Article	IF	CITATIONS
163	Improved tensor based registration: An heterogeneous approach. , 2012, , .		Ο
164	The average cerebral perfusion in patients with multiple sclerosis (MS) using MRI. , 2012, , .		1
165	Effects of variable blast pressures on blood flow and oxygen saturation in rat brain as evidenced using MRI. Magnetic Resonance Imaging, 2012, 30, 527-534.	1.8	30
166	Susceptibility Weighted Imaging and MR Angiography. , 2012, , 157-167.		0
167	Development of a Research Agenda for Evaluation of Interventional Therapies for Chronic Cerebrospinal Venous Insufficiency: Proceedings from a Multidisciplinary Research Consensus Panel. Journal of Vascular and Interventional Radiology, 2011, 22, 587-593.	0.5	14
168	Differential effects of age and history of hypertension on regional brain volumes and iron. NeuroImage, 2011, 54, 750-759.	4.2	63
169	Cortical calcification in sturge–weber syndrome on MRIâ€5WI: Relation to brain perfusion status and seizure severity. Journal of Magnetic Resonance Imaging, 2011, 34, 791-798.	3.4	57
170	Susceptibility weighted imaging in detecting hemorrhage in acute cervical spinal cord injury. Magnetic Resonance Imaging, 2011, 29, 365-373.	1.8	65
171	Semiautomated detection of cerebral microbleeds in magnetic resonance images. Magnetic Resonance Imaging, 2011, 29, 844-852.	1.8	101
172	Mapping of Cerebral Oxygen Extraction Fraction Changes with Susceptibility-weighted Phase Imaging. Radiology, 2011, 261, 930-936.	7.3	39
173	Recent Developments in Imaging of Multiple Sclerosis. Neurologist, 2011, 17, 185-204.	0.7	63
174	Chronic cerebral spinal venous insufficiency in multiple sclerosis. Expert Review of Neurotherapeutics, 2011, 11, 5-9.	2.8	31
175	Chronic cerebrospinal venous insufficiency in multiple sclerosis: a historical perspective. Functional Neurology, 2011, 26, 181-95.	1.3	15
176	Correlation of hypointensities in susceptibility-weighted images to tissue histology in dementia patients with cerebral amyloid angiopathy: a postmortem MRI study. Acta Neuropathologica, 2010, 119, 291-302.	7.7	246
177	Detection of normal spinal veins by using susceptibilityâ€weighted imaging. Journal of Magnetic Resonance Imaging, 2010, 31, 32-38.	3.4	21
178	Imaging cerebral microbleeds using susceptibility weighted imaging: One step toward detecting vascular dementia. Journal of Magnetic Resonance Imaging, 2010, 31, 142-148.	3.4	132
179	Common data elements in radiologic imaging of traumatic brain injury. Journal of Magnetic Resonance Imaging, 2010, 32, 516-543.	3.4	139
180	Correlation of putative iron content as represented by changes in R2* and phase with age in deep gray matter of healthy adults. Journal of Magnetic Resonance Imaging, 2010, 32, 561-576.	3.4	112

#	Article	IF	CITATIONS
181	Quantification of punctate iron sources using magnetic resonance phase. Magnetic Resonance in Medicine, 2010, 63, 106-115.	3.0	39
182	Visualizing Iron Deposition in Multiple Sclerosis Cadaver Brains. , 2010, , .		4
183	Spinal Arteriovenous Malformation: Evaluation of Change in Venous Oxygenation with Susceptibility-weighted MR Imaging after Treatment. Radiology, 2010, 254, 891-899.	7.3	18
184	Quantitative Analysis of Clinical Dynamic Contrast-enhanced MR Imaging for Evaluating Treatment Response in Human Breast Cancer. Radiology, 2010, 257, 47-55.	7.3	33
185	Common Data Elements in Radiologic Imaging of Traumatic Brain Injury. Archives of Physical Medicine and Rehabilitation, 2010, 91, 1661-1666.	0.9	214
186	Dynamic Contrast-Enhanced Magnet Resonance Imaging of Sunitinib-Induced Vascular Changes to Schedule Chemotherapy in Renal Cell Carcinoma Xenograft Tumors. Translational Oncology, 2010, 3, 293-306.	3.7	20
187	Quantifying effective magnetic moments of narrow cylindrical objects in MRI. Physics in Medicine and Biology, 2009, 54, 7025-7044.	3.0	17
188	Identification of calcification with MRI using susceptibilityâ€weighted imaging: A case study. Journal of Magnetic Resonance Imaging, 2009, 29, 177-182.	3.4	223
189	Characterizing iron deposition in multiple sclerosis lesions using susceptibility weighted imaging. Journal of Magnetic Resonance Imaging, 2009, 29, 537-544.	3.4	288
190	Removing background phase variations in susceptibilityâ€weighted imaging using a fast, forwardâ€field calculation. Journal of Magnetic Resonance Imaging, 2009, 29, 937-948.	3.4	76
191	Diminished visibility of cerebral venous vasculature in multiple sclerosis by susceptibilityâ€weighted imaging at 3.0 Tesla. Journal of Magnetic Resonance Imaging, 2009, 29, 1190-1194.	3.4	108
192	Settling properties of venous blood demonstrated in the peripheral vasculature using susceptibilityâ€weighted imaging (SWI). Journal of Magnetic Resonance Imaging, 2009, 29, 1465-1470.	3.4	6
193	Imaging the vessel wall in major peripheral arteries using susceptibilityâ€weighted imaging. Journal of Magnetic Resonance Imaging, 2009, 30, 357-365.	3.4	45
194	MAgnitude and PHase Thresholding (MAPHT) of noisy complex-valued magnetic resonance images. Magnetic Resonance Imaging, 2009, 27, 1271-1280.	1.8	4
195	Principles, Techniques, and Applications of T2*-based MR Imaging and Its Special Applications. Radiographics, 2009, 29, 1433-1449.	3.3	544
196	Limitations of calculating field distributions and magnetic susceptibilities in MRI using a Fourier based method. Physics in Medicine and Biology, 2009, 54, 1169-1189.	3.0	75
197	Dynamic Contrast-Enhanced Magnetic Resonance Imaging of Vascular Changes Induced by Sunitinib in Papillary Renal Cell Carcinoma Xenograft Tumors. Neoplasia, 2009, 11, 910-920.	5.3	54
198	Susceptibility-Weighted Imaging: Clinical Angiographic Applications. Magnetic Resonance Imaging Clinics of North America, 2009, 17, 47-61.	1.1	97

#	Article	IF	CITATIONS
199	Serial Susceptibility Weighted MRI Measures Brain Iron and Microbleeds in Dementia. Journal of Alzheimer's Disease, 2009, 17, 599-609.	2.6	120
200	Advances in neuroimaging of traumatic brain injury and posttraumatic stress disorder. Journal of Rehabilitation Research and Development, 2009, 46, 717.	1.6	80
201	MR susceptibility weighted imaging (SWI) complements conventional contrast enhanced T1 weighted MRI in characterizing brain abnormalities of Sturgeâ€Weber Syndrome. Journal of Magnetic Resonance Imaging, 2008, 28, 300-307.	3.4	89
202	Complex threshold method for identifying pixels that contain predominantly noise in magnetic resonance images. Journal of Magnetic Resonance Imaging, 2008, 28, 727-735.	3.4	34
203	An iterative reconstruction technique for geometric distortion-corrected segmented echo-planar imaging. Magnetic Resonance Imaging, 2008, 26, 1406-1414.	1.8	16
204	Detection of Hemorrhagic Hypointense Foci in the Brain on Susceptibility-Weighted Imaging. Academic Radiology, 2007, 14, 1011-1019.	2.5	78
205	New algorithm for quantifying vascular changes in dynamic contrastâ€enhanced MRI independent of absolute <i>T</i> ₁ values. Magnetic Resonance in Medicine, 2007, 58, 463-472.	3.0	65
206	Dependence of vessel area accuracy and precision as a function of MR imaging parameters and boundary detection algorithm. Journal of Magnetic Resonance Imaging, 2007, 25, 1226-1234.	3.4	21
207	Establishing a baseline phase behavior in magnetic resonance imaging to determine normal vs. abnormal iron content in the brain. Journal of Magnetic Resonance Imaging, 2007, 26, 256-264.	3.4	237
208	A complex sum method of quantifying susceptibilities in cylindrical objects: the first step toward quantitative diagnosis of small objects in MRI. Magnetic Resonance Imaging, 2007, 25, 1171-1180.	1.8	19
209	Biocompatibilities of sapphire and borosilicate glass as cortical neuroprostheses. Magnetic Resonance Imaging, 2007, 25, 1333-1340.	1.8	14
210	A simplified formula for T1 contrast optimization for short-TR steady-state incoherent (spoiled) gradient echo sequences. Magnetic Resonance Imaging, 2007, 25, 1397-1401.	1.8	9
211	Brain Aging and Its Modifiers: Insights from in Vivo Neuromorphometry and Susceptibility Weighted Imaging. Annals of the New York Academy of Sciences, 2007, 1097, 84-93.	3.8	149
212	In vivo measurement of tissue damage, oxygen saturation changes and blood flow changes after experimental traumatic brain injury in rats using susceptibility weighted imaging. Magnetic Resonance Imaging, 2007, 25, 219-227.	1.8	82
213	The role of voxel aspect ratio in determining apparent vascular phase behavior in susceptibility weighted imaging. Magnetic Resonance Imaging, 2006, 24, 155-160.	1.8	85
214	Susceptibility-weighted imaging to visualize blood products and improve tumor contrast in the study of brain masses. Journal of Magnetic Resonance Imaging, 2006, 24, 41-51.	3.4	184
215	Susceptibility Weighted Imaging (SWI). Zeitschrift Fur Medizinische Physik, 2006, 16, 237.	1.5	17
216	Clinical applications of neuroimaging with susceptibilityâ€weighted imaging. Journal of Magnetic Resonance Imaging, 2005, 22, 439-450.	3.4	404

#	Article	IF	CITATIONS
217	Nonnvasive assessment of vascular architecture and function during modulated blood oxygenation using susceptibility weighted magnetic resonance imaging. Magnetic Resonance in Medicine, 2005, 54, 87-95.	3.0	130
218	Imaging iron stores in the brain using magnetic resonance imaging. Magnetic Resonance Imaging, 2005, 23, 1-25.	1.8	891
219	Reliability in detection of hemorrhage in acute stroke by a new threeâ€dimensional gradient recalled echo susceptibilityâ€weighted imaging technique compared to computed tomography: A retrospective study. Journal of Magnetic Resonance Imaging, 2004, 20, 372-377.	3.4	138
220	Susceptibility weighted imaging (SWI). Magnetic Resonance in Medicine, 2004, 52, 612-618.	3.0	1,480
221	Hemorrhagic Shearing Lesions in Children and Adolescents with Posttraumatic Diffuse Axonal Injury: Improved Detection and Initial Results. Radiology, 2003, 227, 332-339.	7.3	392
222	Quantification of errors in volume measurements of the caudate nucleus using magnetic resonance imaging. Journal of Magnetic Resonance Imaging, 2002, 15, 353-363.	3.4	11
223	Partial Fourier imaging in multi-dimensions: A means to save a full factor of two in time. Journal of Magnetic Resonance Imaging, 2001, 14, 628-635.	3.4	33
224	High-resolution BOLD venographic imaging: a window into brain function. NMR in Biomedicine, 2001, 14, 453-467.	2.8	232
225	Predicting BOLD signal changes as a function of blood volume fraction and resolution. NMR in Biomedicine, 2001, 14, 468-477.	2.8	32
226	A current perspective of the status of understanding BOLD imaging and its use in studying brain function: a summary of the workshop at the University of North Carolina in Chapel Hill, 26-28 October, 2000. NMR in Biomedicine, 2001, 14, 384-388.	2.8	6
227	High-Resolution MR Venography at 3.0 Tesla. Journal of Computer Assisted Tomography, 2000, 24, 949-957.	0.9	190
228	Sub-millimeter fMRI at 1.5 tesla: Correlation of high resolution with low resolution measurements. Journal of Magnetic Resonance Imaging, 1999, 9, 475-482.	3.4	47
229	Accuracy of T1 measurements at high temporal resolution: Feasibility of dynamic measurement of blood T1 after contrast administration. Journal of Magnetic Resonance Imaging, 1999, 10, 576-581.	3.4	27
230	Efficacy of slow infusion of gadolinium contrast agent in three-dimensional MR coronary artery imaging. Journal of Magnetic Resonance Imaging, 1999, 10, 800-805.	3.4	33
231	Geometric distortion correction in gradient-echo imaging by use of dynamic time warping. Magnetic Resonance in Medicine, 1999, 42, 585-590.	3.0	25
232	Geometric distortion correction in gradientâ€echo imaging by use of dynamic time warping. Magnetic Resonance in Medicine, 1999, 42, 585-590.	3.0	1
233	In vivo measurement of changes in venous blood-oxygenation with high resolution functional MRI at 0.95 Tesla by measuring changes in susceptibility and velocity. Magnetic Resonance in Medicine, 1998, 39, 97-107.	3.0	76
234	Accurate determination of spin-density andT1 in the presence of RF-field inhomogeneities and flip-angle miscalibration. Magnetic Resonance in Medicine, 1998, 40, 592-602.	3.0	136

#	Article	IF	CITATIONS
235	High-resolution venography of the brain using magnetic resonance imaging. Magnetic Resonance Materials in Physics, Biology, and Medicine, 1998, 6, 62-69.	2.0	106
236	Contrast-enhanced magnetic resonance angiography of carotid arterial wall in pigs. Journal of Magnetic Resonance Imaging, 1997, 7, 183-190.	3.4	62
237	Theory and application of static field inhomogeneity effects in gradient-echo imaging. Journal of Magnetic Resonance Imaging, 1997, 7, 266-279.	3.4	254
238	Quantitation ofT2′ anisotropic effects on magnetic resonance bone mineral density measurement. Magnetic Resonance in Medicine, 1997, 37, 214-221.	3.0	54
239	An MRI method for measuringT2 in the presence of static and RF magnetic field Inhomogeneities. Magnetic Resonance in Medicine, 1997, 37, 872-876.	3.0	82
240	Quantitative regional brain water measurement with magnetic resonance imaging in a focal ischemia model. Magnetic Resonance in Medicine, 1997, 38, 303-310.	3.0	36
241	Quantitative measurements of regional cerebral blood volume using MRI in rats: Effects of arterial carbon dioxide tension and mannitol. Magnetic Resonance in Medicine, 1997, 38, 420-428.	3.0	58
242	Role of high resolution in magnetic resonance (MR) imaging: Applications to MR angiography, intracranialT1-weighted imaging, and image interpolation. International Journal of Imaging Systems and Technology, 1997, 8, 529-543.	4.1	36
243	In vivo measurement of blood oxygen saturation using magnetic resonance imaging: A direct validation of the blood oxygen level-dependent concept in functional brain imaging. Human Brain Mapping, 1997, 5, 341-346.	3.6	198
244	Magnetic resonance imaging of the brain with gadopentetate dimeglumine-DTPA: Comparison of T1-weighted spin-echo and 3D gradient-echo sequences. Journal of Magnetic Resonance Imaging, 1996, 6, 415-424.	3.4	37
245	Functional MRI in human somatosensory cortex activated by touching textured surfaces. Journal of Magnetic Resonance Imaging, 1996, 6, 565-572.	3.4	72
246	Adaptive blood pool segmentation in three-dimensions: Application to MR cardiac evaluation. Journal of Magnetic Resonance Imaging, 1996, 6, 690-697.	3.4	11
247	Assessment of cerebral blood flow reserve using functional magnetic resonance imaging. Journal of Magnetic Resonance Imaging, 1996, 6, 718-725.	3.4	31
248	Improving the temporal resolution of functional MR imaging using keyhole techniques. Magnetic Resonance in Medicine, 1996, 35, 854-860.	3.0	47
249	Myocardial signal response to dipyridamole and dobutamine: Demonstration of the BOLD effect using a double-echo gradient-echo sequence. Magnetic Resonance in Medicine, 1996, 36, 16-20.	3.0	119
250	Commutator filter: A novel technique for the identification of structures producing significant susceptibility inhomogeneities and its application to functional MRI. Magnetic Resonance in Medicine, 1996, 36, 781-787.	3.0	18
251	In vivo validation of the bold mechanism: A review of signal changes in gradient echo functional MRI in the presence of flow. International Journal of Imaging Systems and Technology, 1995, 6, 153-163.	4.1	99
252	Carotid plaque formation and its evaluation with angiography, ultrasound, and MR angiography. Journal of Magnetic Resonance Imaging, 1994, 4, 515-527.	3.4	30

#	Article	IF	CITATIONS
253	Three-dimensional time-of-flight MR angiography using selective inversion recovery RAGE with fat saturation and ECG-triggering: Application to renal arteries. Magnetic Resonance in Medicine, 1994, 31, 414-422.	3.0	49
254	Three-dimensional time-of-flight MR angiography with variable TE (VARIETE) for fat signal reduction. Magnetic Resonance in Medicine, 1994, 32, 678-683.	3.0	9
255	Theory of NMR signal behavior in magnetically inhomogeneous tissues: The static dephasing regime. Magnetic Resonance in Medicine, 1994, 32, 749-763.	3.0	1,086
256	Basic physics of MR contrast agents and maximization of image contrast. Journal of Magnetic Resonance Imaging, 1993, 3, 137-148.	3.4	131
257	Three-dimensional MR imaging of the coronary arteries: Preliminary clinical experience. Journal of Magnetic Resonance Imaging, 1993, 3, 491-500.	3.4	74
258	Gadolinium-enhanced high-resolution MR angiography with adaptive vessel tracking: Preliminary results in the intracranial circulation. Journal of Magnetic Resonance Imaging, 1992, 2, 277-284.	3.4	68
259	A future outlook for the SMRI: Perspective of the past president. Journal of Magnetic Resonance Imaging, 1992, 2, 375-376.	3.4	Ο
260	Automated local maximum-intensity projection with three-dimensional vessel tracking. Journal of Magnetic Resonance Imaging, 1992, 2, 519-526.	3.4	24
261	Modified iterative model based on data extrapolation method to reduce Gibbs ringing. Journal of Magnetic Resonance Imaging, 1991, 1, 307-317.	3.4	25
262	Lumen definition in MR angiography. Journal of Magnetic Resonance Imaging, 1991, 1, 327-336.	3.4	16
263	A guide to understanding key aspects of fast gradient-echo imaging. Journal of Magnetic Resonance Imaging, 1991, 1, 621-624.	3.4	18
264	Phase-constrained data extrapolation method for reduction of truncation artifacts. Journal of Magnetic Resonance Imaging, 1991, 1, 721-724.	3.4	11
265	Carotid-CNS MR flow imaging. Magnetic Resonance in Medicine, 1990, 14, 308-314.	3.0	36
266	Constrained reconstruction: A superresolution, optimal signal-to-noise alternative to the Fourier transform in magnetic resonance imaging. Medical Physics, 1989, 16, 388-397.	3.0	60
267	Pseudo-gating: Elimination of periodic motion artifacts in magnetic resonance imaging without gating. Magnetic Resonance in Medicine, 1987, 4, 162-174.	3.0	66
268	Susceptibility-weighted imaging in traumatic brain injury. , 0, , 691-704.		1
269	Susceptibility-weighted imaging. , 0, , 129-136.		Ο
270	Susceptibility-weighted imaging. , 0, , 22-33.		3

#	Article	IF	CITATIONS
271	Appendix: Seminal Articles Related to the Development of Susceptibility Weighted Imaging. , 0, , 697-716.		0